*Journal of Applied Mechanics and Technical Physics, Vol. 43, No. 2, pp. 280–285, 2002*

# CAVITIES BEHIND A SPILLWAY WITH A WIDE SILL

**V. I. Bukreev and A. V. Gusev**

UDC 532.59

*The paper reports experimental results on flow regimes with and without cavities behind a rectangular sill in an open channel. Photographs illustrating the shapes of the free ends of the cavities are given. It is shown that the domains of existence of various flow regimes overlap in the phase space of problem parameters, which leads to nonuniqueness of various functions of the parameters. Quantitative information is obtained for free surface profiles, the discharge coefficient, and the pressure on the flow bottom.*

**Introduction.** We consider the following two-dimensional steady flow. In a rectangular open channel of width $B$ and zero bottom slope there is a rectangular sill of length $l$, height $b$, and width greater than the width of the channel. The volumetric discharge $Q = \text{const}$ and the tail-water depth $h_+$ are specified. If the incident flow is supercritical [1], the head-water depth $h_-$ is an independent external parameter. Among physical constants, the most important for this work are the acceleration of gravity $g$ and the coefficient of surface tension $\sigma$. We use a fixed Cartesian coordinate system in which the longitudinal coordinate $x$ is directed downstream and is reckoned from the downstream edge of the sill, and the vertical coordinate of the free surface $\eta$ is reckoned from the channel bottom. In conversion to dimensionless quantities, the critical depth $h_* = (q^2/g)^{1/3}$ ($q = Q/B$ is the specific discharge) is used as the characteristic linear scale. The pressure $p$ is normalized to $\rho g h_*$ ($\rho$ is the liquid density). The superscript 0 denotes dimensionless quantities.

Flow separation from the upstream and downstream edges of the sill and the possibility of discontinuity of the liquid imply the existence of a few dozens of different flow regimes in the phase space of the indicated parameters. The regions of existence of these regimes overlap in a complex manner [1, 2]. Moreover, in some processes a hysteresis is observed when the transition from one regime to another occurs at different values of parameters, depending on the direction of motion of the image point along the corresponding trajectory of the phase space [3]. Although this type of flow has been extensively studied [see, for example, (1–4)], some questions remain to be studied, in particular, the range of parameters in which formation of air cavities is possible. The present paper studies this range of parameters. Experimental results given in [5] were obtained for another range of parameters using the same sill as in the present work.

The experiments showed that cavities can form not only behind the sill but also over the sill as a result of flow separation from the upstream edge of the sill. Below, we consider only the cavities formed behind the sill. The cavities formed over the sill are rather complex and require separate investigation. Their unique feature is that an air cavity can be formed at a long distance from rigid flow boundaries. As a rule, these cavities are unstable and can exist only when the incident flow is supercritical ($h_-^0 < 1$).

Experimental studies of cavities behind a sill use simple methods (including visual observation) and yield information on the stability and shapes of the free ends of the cavities, which is necessary for their adequate mathematical simulation [6]. In addition, the effects associated with surface tension have attracted much attention in recent hydrodynamic studies. The role of interphase tension in the linear theory of stability has been studied in great detail [7]. Longuet-Higgins [8] investigated theoretically the effect of surface tension on nonlinear waves of ultimate steepness. An important direction is the investigation of flows under low gravity, where surface tension and its dependence on temperature become governing factors [9]. Cavities behind a sill can be used as reliable objects for testing various mathematical models that take into account surface tension and cohesion forces at the contact boundary between a liquid, a gas, and a solid.

Lavrent'ev Institute of Hydrodynamics, Siberian Division, Russian Academy of Sciences, Novosibirsk 630090.
Translated from Prikladnaya Mekhanika i Tekhnicheskaya Fizika, Vol. 43, No. 2, pp. 129–135, March–April, 2002. Original article submitted October 17, 2001.

 0021-8944/02/4302-0280 $27.00 

A special feature of the flow considered is that the same values of external parameters can yield different regimes of liquid motion, for example, motions with clinging, depressed, or free nappes [1]. In hydraulics there is no common term to describe this phenomenon. In the present paper, we use the term of "nonuniqueness of flow." In the nonuniqueness region, the free surface level, rate, pressure, the discharge coefficient, and other quantities are multiple valued functions of the parameters of the problem. Usually, the regimes with clinging, depressed, or free nappes are described qualitatively by the problem of a sharp-crested spillway [1, 4]. In the present paper, quantitative and qualitative information is obtained for a spillway with a wide sill. The meaning of the term of "wide sill" is clarified in [1]. We note that the regime with cavities is a particular case of the free-nappe regime where an air cavity under the nappe is closed, i. e., does not communicate with the atmosphere.

**Experimental Method.** The experiments were performed in a channel of length 4.8 m and width $B = 6$ cm. The examples given below were obtained for a sill with a length of $l = 30$ cm and a height of $b = 4.85$ cm. The sill and the channel bottom and walls were made of Plexiglas. As the working liquid, we used tap water purified from impurities and dissolved air at a temperature of 15–18°C. The error of the parameters of the problem was less than 1%. To identify the flow regimes and determine their stability, we introduced fine aluminum particles to make the internal flow structure visible. Using photographs with $\times 2$ magnification, we measured the vertical coordinate of the free surface $\eta$ reckoned from the channel bottom (the absolute error did not exceed $\pm 0.5$ mm). The pressure $p$ along the longitudinal symmetry axis of the channel bottom was measured with piezometers with an absolute error less than $\pm 0.2$ Pa.

Due to the so-called nonuniqueness of the flow, for the same values of external parameters, we can obtain not only steady regimes with or without a cavity but also a continuous set of regimes with cavities of various volumes. In the experiments, various methods for controlling the volume of cavities were used. One of these methods involved selection of the rate of discharge variation from zero to a specified constant value. If a steady regime was reached slowly, there was a continuous transition from the clinging-nappe regime to the depressed-nappe regime without cavities. If the discharge increased very rapidly, an unstable cavity first formed. After some time, the cavity volume decreased until one of stable configurations was formed due to the development of air bubbles.

For a steady-state discharge, transition from the clinging-nappe regime to the depressed-nappe regime with cavities of different volumes (in the region of their existence) was implemented by dosed supply of air under the nappe (as in the game with soap bubbles). A short-term increase in tail-water level with subsequent return to the specified steady-state conditions was sufficient for reverse transition from the regime with cavities to the clinging-nappe regime. Under certain conditions, the cavity volume can change in a self-oscillating regime, which is accompanied by a loud sound, as is the case "expulsive" waterfalls.

**Examples of Cavities behind the Sill.** In the examples below, the incident flow was subcritical ($h_-^0 > 1$), and the flow behind the sill was supercritical ($h_+^0 < 1$). The experiments showed that in this case, for any combination of parameters of the problem in the region of existence of cavities, there are maximum and minimum air volumes, which can be contained inside the cavity for an infinitely long time. The cavity is called stable if the amount of air enclosed in it (virtually, the entire volume) does not change for an infinitely long time. In this case, a regular or chaotic change in the cavity shape with time is admitted. Observations showed that the form of the free end of the cavity changes most significantly. The upper and lower boundaries fluctuate even in stable cavities but these fluctuations are more regular and weaker than those of the boundary of the cavity free end.

For cavities over the sill, the main destabilizing factors are the friction force and the buoyancy force due to the difference between the air and water densities. The surface tension on the cavity boundaries and the cohesion force at the "water–gas–rigid wall" interface have a stabilizing effect. Depending on the combination of parameters of the problem, the pressure distribution over the cavity surface can be either a stabilizing or destabilizing factor. As a result, three mechanisms of stability loss were observed in the experiments.

In the "mild" mechanism of stability loss, individual air bubbles were carried away from the free cavity end by the flow until a stable cavity of maximum volume formed for the specified combination of parameters. In the second mechanism, stability was affected primarily by fluctuations of the upper and lower boundaries of the cavity. If the amplitude of the fluctuations was larger than the cavity thickness, the upper and lower cavity boundaries merged, and the cavity disintegrated into separate air bubbles and then disappeared. This loss of stability is typical of cavities of minimum volume at specified combination of parameters. The third mechanism was observed when the tail-water level exceeded a certain threshold value and the pressure distribution over the cavity boundaries was such that destabilizing factors became dominant. In this case, the cavity collapsed irrespective of its initial volume.

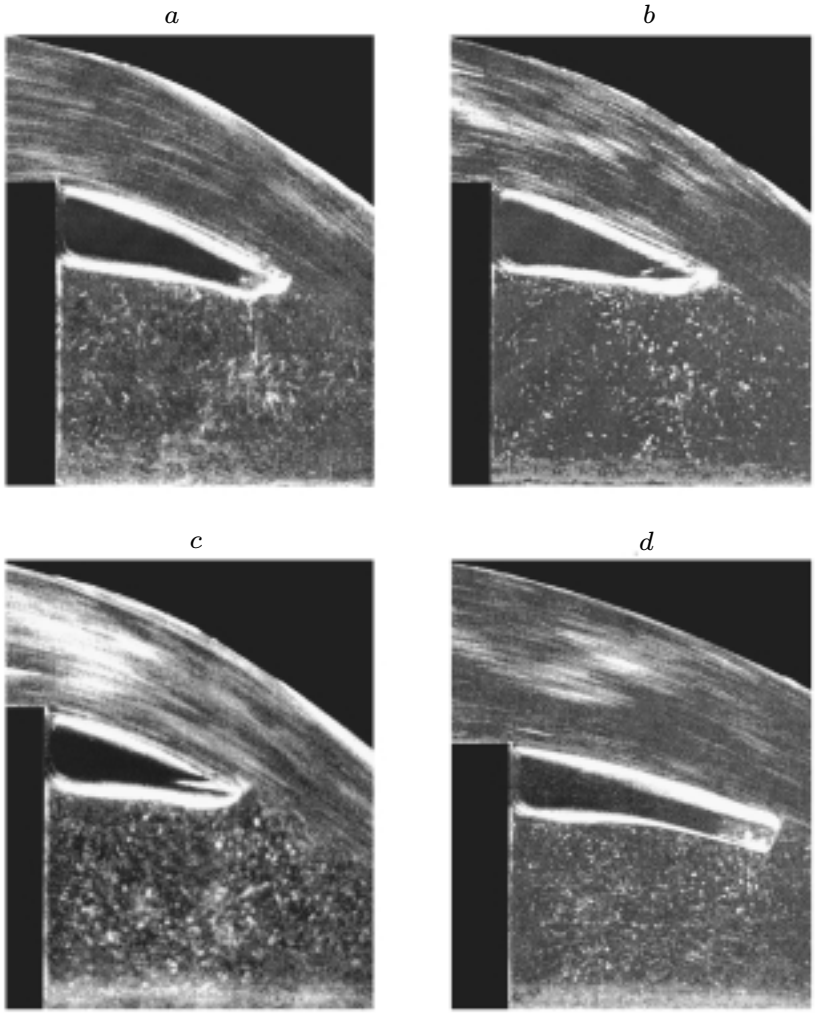


Fig. 1. Shapes of the free ends of stable and unstable cavities: (a) unstable cavity for $h_* = 2.85$ cm; (b) stable cavity of maximum volume for $h_* = 2.85$ cm; (c) stable cavity with a return nappe for $h_* = 2.85$ cm; (d) unstable cavity with a flat free end for $h_* = 3.95$ cm.

Figure 1 shows examples of stable and unstable cavities. The cavity in Fig. 1a is unstable. It formed when the steady regime was reached rapidly, and it was recorded when rare air bubbles still emerged. With time, this cavity transformed into a stable cavity with a maximum volume possible for the specified combination of parameters (Fig. 1b). The cavity in Fig. 1c is also stable and was obtained at constant values of the parameters by artificial suction of air from the cavity shown in Fig. 1b. A special feature of this cavity is that there is a return nappe at its free end.

Within the model of an ideal liquid with standard boundary conditions, the cavity length is infinitely great [6]. A number of heuristic methods were proposed to eliminate this paradox [6]. A more suitable model is the Riabouchinsky–Weinig calculation scheme, which uses an imaginary return nappe [6]. In contrast to an imaginary nappe (see [6]), the shape and size of a real return nappe (Fig. 1c) change continuously. In addition, there are stable cavities (see Fig. 1b and Fig. 2b) that have no distinct return nappe. However, the main idea of the calculation scheme that a portion of perturbation energy can return from infinity into a cavity was supported by our experiments.

In another calculation scheme, the free end of a cavity is closed by an imaginary plate [6]. The photograph shown in Fig. 1d illustrates the existence of this shape of the free end in real cavities. However, our experiments showed that cavities with a flat free end are unstable. In particular, the cavity in Fig. 1d is unstable in accordance with the "mild" mechanism described above. A flat free end is also observed in some cavities that are unstable according to the second mechanism described above.

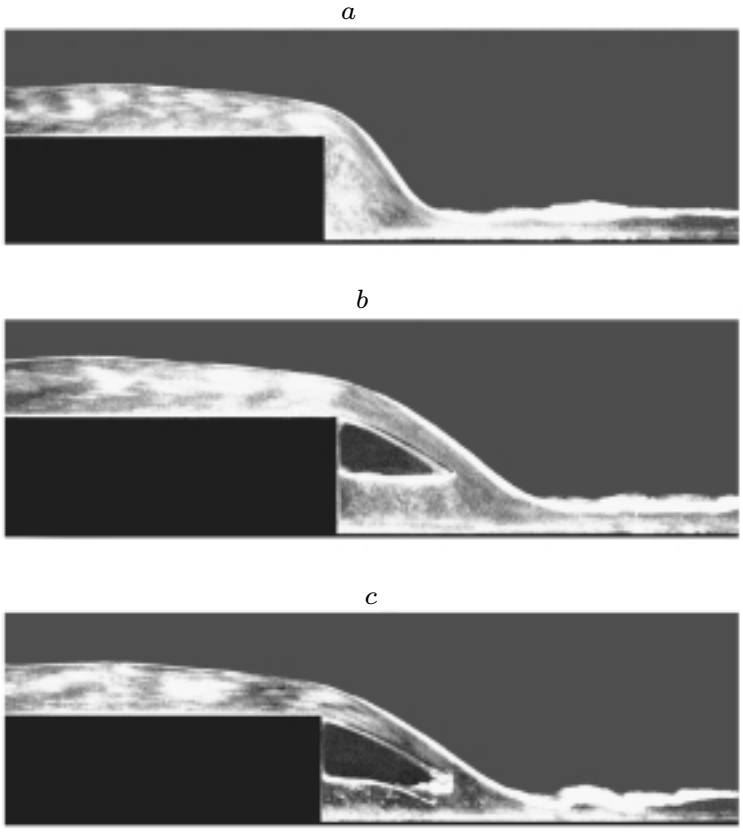


Fig. 2. Different flow regimes for $h_* = 1.98$ cm: (a) depressed nappe; (b) stable cavity; (c) unstable cavity.

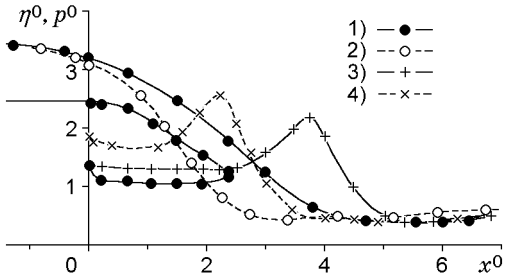


Fig. 3. Free surface profiles and pressure distributions over the channel bottom for $h_* = 1.98$ cm: curve 1 refers to $\eta_k^0$, curve 2 to $\eta^0$, curve 3 to $p_k^0$, and curve 4 to $p^0$.

**Nonuniqueness of Flow.** The photographs shown in Fig. 1a–c were obtained for the same values of external parameters, although the flow patterns recorded differ greatly from each other. Another example of such "nonuniqueness" obtained for another combination of external parameters is shown in Fig. 2. A steady flow pattern without a cavity formed when the discharge was varied slowly from zero to a certain constant value (Fig. 2a). According to [1], such flow is called "the depressed-nappe regime." Additional injection of air under the nappe at a constant discharge led to the formation of cavities of various shapes and volumes. Two of these cavities are shown in Fig. 2b and c. The cavity in Fig. 2b is stable. Its free end has the shape of an acute angle smoothed by surface tension. The cavity in Fig. 2c is unstable in accordance with the "mild" mechanism.

The presence or absence of a cavity for the same values of external parameters leads to a significant change in the free surface profile $\eta(x)$ and the pressure at the channel bottom $p(x)$. Figure 3 shows experimental results for a stable cavity of maximum volume. Curves 1 and 3 show curves of $\eta_k^0(x^0)$ and $p_k^0(x^0)$ in the presence of a

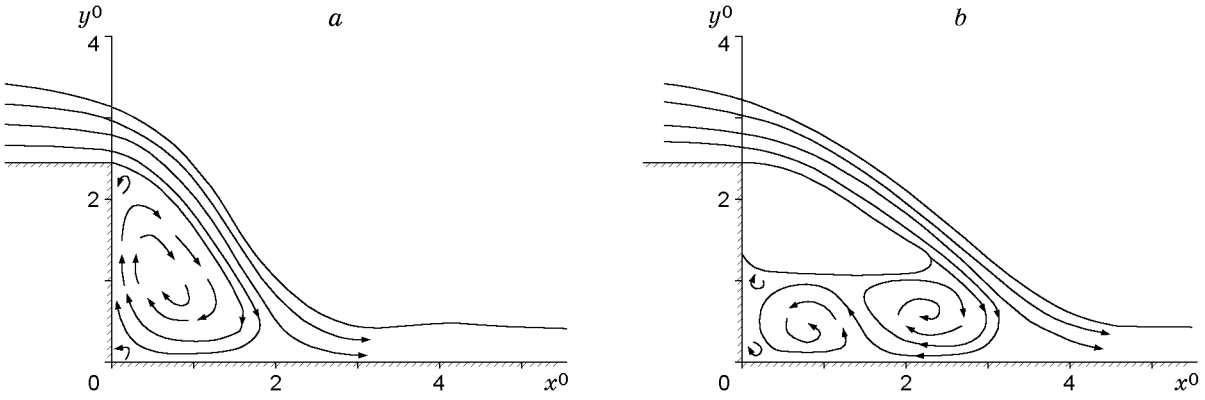


Fig. 4. Streamlines for $h_* = 1.98$ cm in the absence of a cavity (a) and presence of a cavity (b).

cavity, and curves 2 and 4 show curves of $\eta^0(x^0)$ and $p^0(x^0)$ in the absence of a cavity. In this case, the pressure inside the cavity is higher than atmospheric pressure by approximately 10 Pa. However, the lower cavity boundary is above the tail-water level. In the range of $0 < x^0 < 2.4$, which is equal to the cavity length, the function $\eta_k^0$ has three values. In this range, the pressure $p_k^0$ is constant and less than the hydrostatic pressure. The pressure $p_k^0$ becomes equal to the hydrostatic pressure outside the cavity (for $x^0 \approx 2.8$). For $x^0 = 3.8$, the quantity $p_k^0$ reaches the maximum due to incidence of the nappe and then decreases to the hydrostatic pressure again.

In the absence of a cavity, the pressure curve $p^0$ is similar to the pressure curve $p_k^0$ but is displaced along the $x^0$ to the coordinate origin (Fig. 3). The maximum $p^0$ exceeds the maximum $p_k^0$ because in the absence of a cavity, the slope of the incident nappe to the channel bottom is greater than that in the presence of a cavity.

Measurements performed for other combinations of parameters revealed the following regularities. In the absence of cavities and for the chosen method of normalization, there is a sufficiently large parameter space in which the maximum of the function $p^0$ is reached in a small neighborhood of the same value of $x^0$ ($x^0 = 2.4 \pm 0.1$). Maximum values of $p^0$ increase monotonically with decrease in the critical depth $h_*$. In the presence of a cavity, the position of the maximum of the function $p_k^0$ on the $x^0$ axis depends strongly on $h_*$ and the size of the cavity. With decrease in $h_*$, the maximum of $p_k^0$ increases and shifts toward larger $x^0$, other conditions being equal. The experiments showed that for a chosen characteristic length scale $h_*$, there is a region in the phase space of parameters in which the pressure at the bottom $p_k^0$ under the cavity depends slightly on $x^0$ and the chosen values of dimensionless parameters.

The presence or absence of cavities have a significant effect on other characteristics of the flow, for example, on the discharge coefficient. In the absence of a cavity, this coefficient has the largest value. In an experiment with a cavity, the discharge coefficient decreased by 10% in comparison with its value obtained in the absence of cavity (other conditions being equal).

Figure 4 shows schematically streamline patterns in the absence and in the presence of a cavity for the same combination of parameters as in Figs. 2 and 3. The formation of a cavity is accompanied by a decrease in the slope of the incident nappe to the channel bottom. In addition, there is a decrease in the mass, momentum, and energy of the portion of the liquid that moves along the bottom to the sill. This results in significant changes in the pattern and intensity of vortices in the stagnation zone under the nappe. In the example considered, in the absence of a cavity, one main vortex of large intensity formed under the nappe. In addition, there are numerous small vortices formed, for example, in the angles between rigid boundaries. In the presence of a cavity, two vortices of a smaller intensity form.

**Discussion of Results.** Because of the wide variety of flow patterns, investigation of the problem of an open-channel flow over a sill is very difficult; on the other hand, it stimulates the development of novel mathematical models. In particular, to describe flows with and without cavities using a unified approach, a mathematical model should contain an element that simulates a "relay" which "switches on" or "switches off" a certain physical mechanism for changing the flow pattern. In addition, it is necessary to describe the conditions for actuation of the "relay."

In the problem considered and in a number of other hydrodynamic problems, the interaction of water molecules, gas particles, and rigid wall is the physical mechanism whose "switching on" or "switching off" leads to changes in the flow pattern. The methods for taking this mechanism into account in mathematical models are well known (see, for example [7, 9]). It may happen that in the problem of cavities behind a sill, the conditions for "relay" operation are described in a simpler manner than in other problems. The information on the rate of attaining a steady regime reported in the present paper could be useful in formulating these conditions.

This work was supported by the Russian Foundation for Fundamental Research (Grant No. 01-01-00846) and the Foundation for Leading Scientific Schools (Grant No. 00-05-98542).

## REFERENCES

1. P. G. Kiselev, *Reference Book on Hydraulic Calculations* [in Russian], Gosénergoizdat, Moscow–Leningrad (1957).
2. Ven Te Chow, *Open-Channel Hydraulics*, McGraw Hill Book Co., New York (1959).
3. S. Wu and N. Rajaratnam, "Impinging jet and surface flow regimes at drop," *J. Hydraul. Res.*, **36**, No. 1, 69–74 (1998).
4. R. R. Chugaev, *Hydraulics* [in Russian], Énergoatomizdat, Leningrad (1982).
5. V. I. Bukreev, "Undular jump in open-channel flow over a sill," *J. Appl. Mech. Tech. Phys.*, **42**, No. 4, 596–602 (2001).
6. G. Birkhoff and E. Zarantonello, *Jets, Wakes and Cavities*, Academic Press, New York (1957).
7. S. A. Thorpe, "Experiments on the stability of stratified shear flow: Immiscible fluids," *J. Fluid Mech.*, **40**, No. 1, 25–48 (1969).
8. M. S. Longuet-Higgins, "Capillary-gravity waves of solitary type on deep water," *J. Fluid Mech.*, **200**, 451–470 (1989).
9. V. V. Pukchnachov, "Thermocapillary convection under low gravity," *Fluid Dyn. Trans.*, **14**, 145–200 (1989).